

## Electronic Supporting Information (ESI)

# Theoretical understanding of oxygen stability in Mn–Fe binary layered oxides for sodium-ion batteries

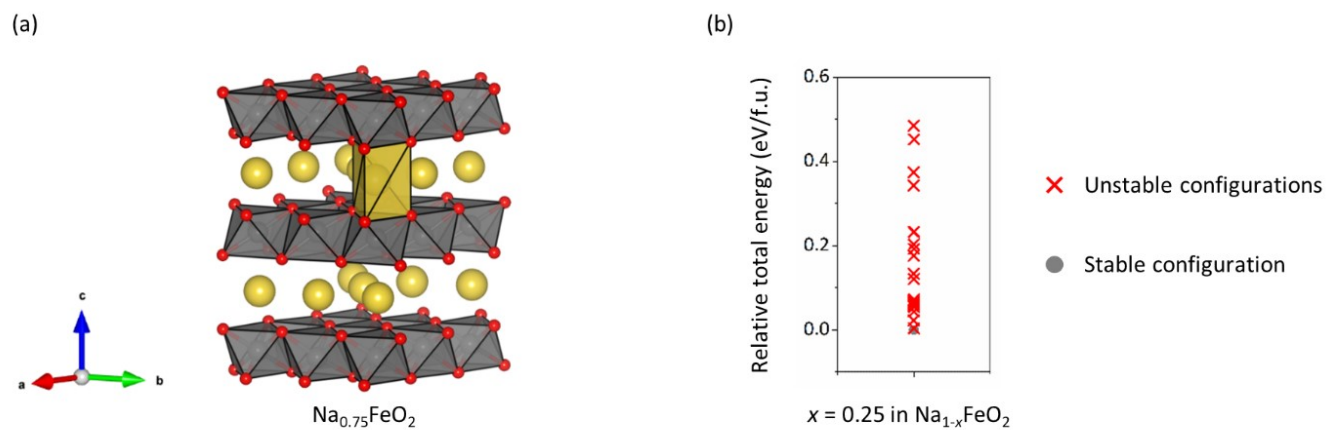
Myungkyu Kim<sup>a,‡</sup>, Hyungjun Kim<sup>a,‡</sup>, Maenghyo Cho<sup>a,\*</sup> and Duho Kim<sup>b,\*</sup>

<sup>a</sup> Department of Mechanical Engineering, Seoul National University, Gwanak-ro 1, Gwanak-gu, Seoul 08826, Republic of Korea

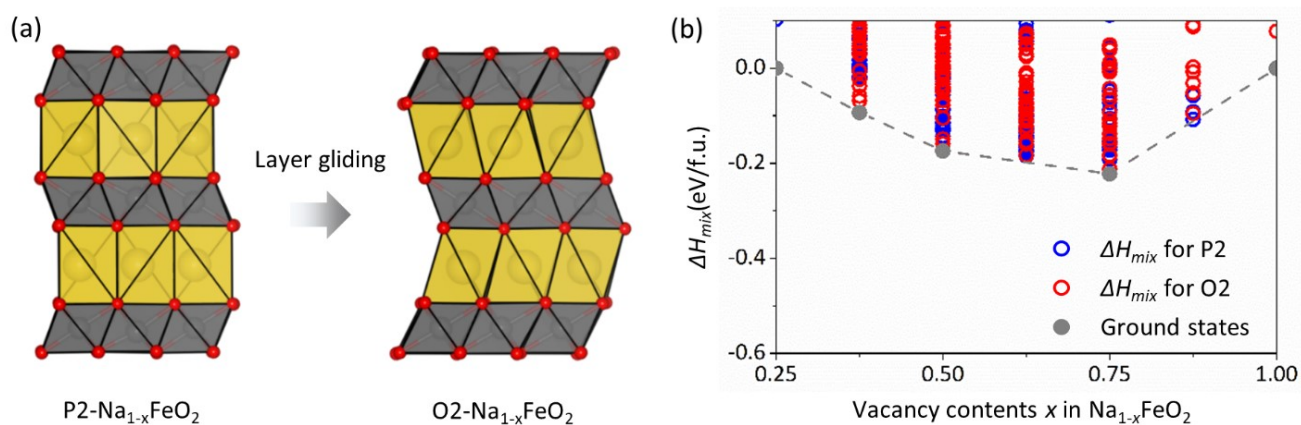
<sup>b</sup> Department of Mechanical Engineering (Integrated Engineering Program), Kyung Hee University, 1732, Deogyong-daero, Giheung-gu, Yongin-si, Gyeonggi-do, 17104, Republic of Korea

<sup>‡</sup> These authors contributed equally

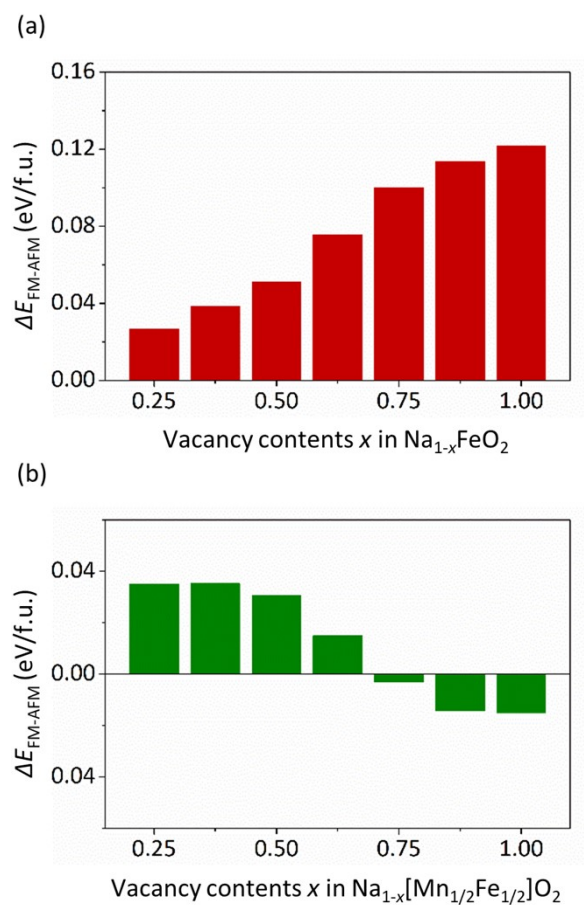
\*Correspondence: [mhcho@snu.ac.kr](mailto:mhcho@snu.ac.kr) (M.Cho), [duhokim@khu.ac.kr](mailto:duhokim@khu.ac.kr) (D.Kim)



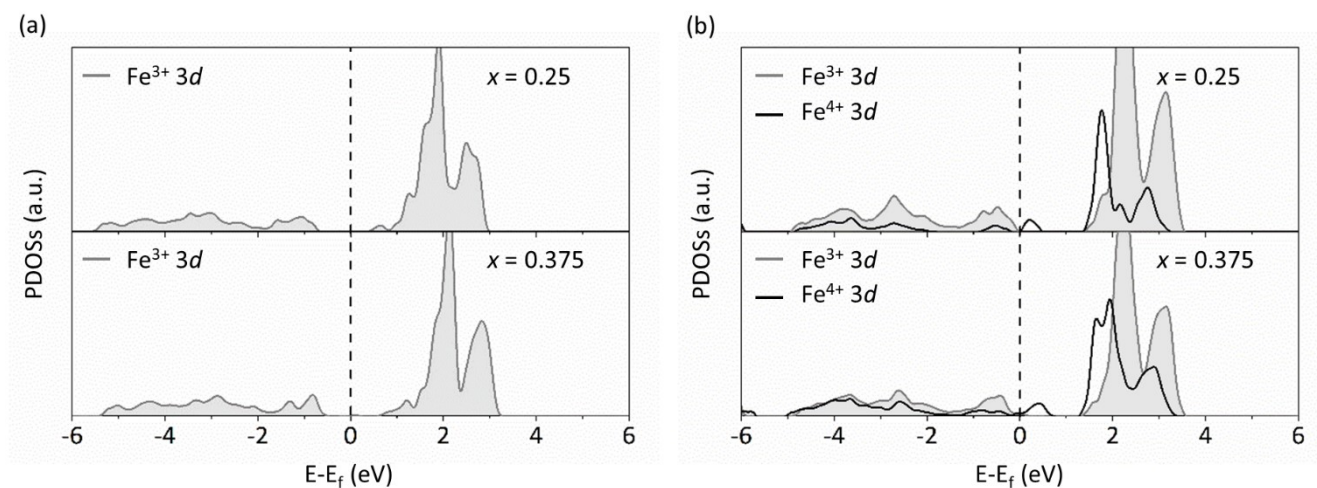
**Figure S1.** (a) An atomic structure of  $\text{Na}_{0.75}\text{FeO}_2$ , which is modeled by referring to the structural information of NMFO.<sup>1</sup> (b) Relative total energies considering all possible Na/vacancy mixed cases at  $x = 0.25$  in  $\text{Na}_{1-x}\text{FeO}_2$  (containing 8 f.u.). Stable configuration (gray filled circle) indicates the ground state structure having the lowest DFT energy.



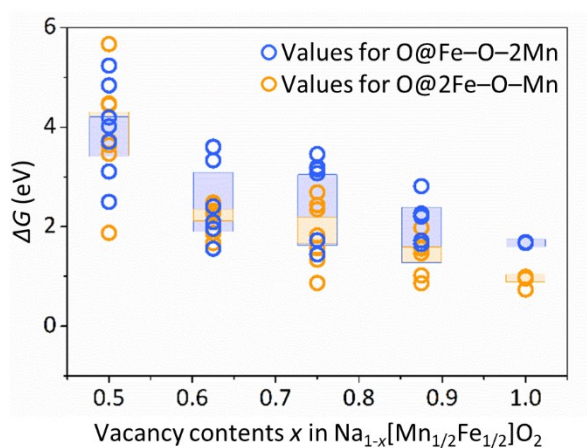
**Figure S2.** (a) The atomic structures of P2-Na<sub>1-x</sub>FeO<sub>2</sub> and O2-Na<sub>1-x</sub>FeO<sub>2</sub> at x = 0.25. The atomic models of pristine O2 stacking NFO were obtained by gliding transition metal slabs by (1/3, 2/3, 0) direction of P2-NFO ground state structure.<sup>2</sup> (b) Convex hull diagram considering possible phase transition during charging process. Filled gray circles on the dashed line indicates the ground states, which means the lowest  $\Delta H_{mix}$  values among values at thermodynamically stable phases determined by convex hull analysis. The rest of the  $\Delta H_{mix}$  values were named according to their stacking sequence of the atomic models.



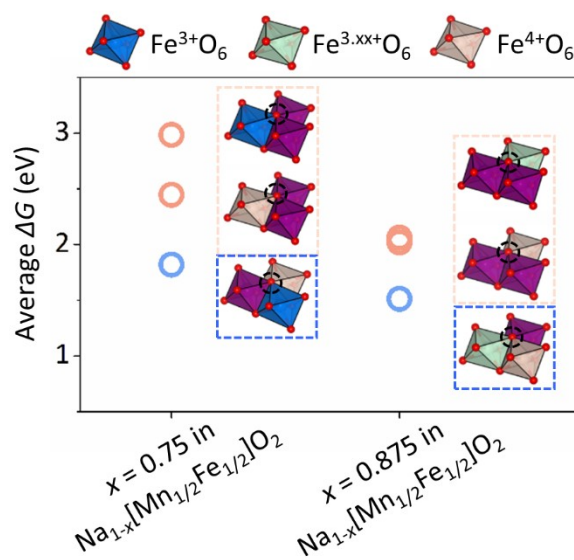
**Figure S3.** Energy difference between the ferromagnetic (FM) and antiferromagnetic (AFM) ( $\Delta E_{\text{FM-AFM}}$ ) of (a)  $\text{Na}_{1-x}\text{FeO}_2$  and (b)  $\text{Na}_{1-x}[\text{Mn}_{1/2}\text{Fe}_{1/2}]\text{O}_2$  in the vacancy range of  $0.25 \leq x \leq 1.0$ . The  $\Delta E_{\text{FM-AFM}} > 0$  indicates that AFM is the energetically favorable spin ordering, whereas negative energy difference ( $\Delta E_{\text{FM-AFM}} < 0$ ) presents that FM is the stable magnetic ordering.



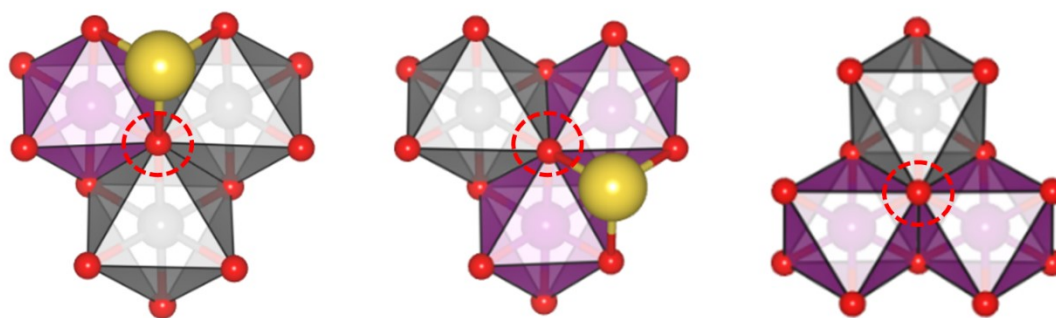
**Figure S4.** Partial density of states (PDOSs) of  $\text{Fe}^{3+}$  (gray) and  $\text{Fe}^{4+}$  (black) 3d-electron at  $x = 0.25$  and  $0.375$  for (a)  $\text{Na}_{1-x}[\text{Mn}_{1/2}\text{Fe}_{1/2}]\text{O}_2$  and (b)  $\text{Na}_{1-x}\text{FeO}_2$ . The change of PDOSs for  $\text{Fe}^{3+}$  in the valence band ( $-1.0 \text{ eV} \leq E-E_f \leq 0.0 \text{ eV}$ ) and those for  $\text{Fe}^{4+}$  in the conduction band ( $0.0 \text{ eV} \leq E-E_f \leq 1.0 \text{ eV}$ ) presents the cationic redox reaction of  $\text{Fe}^{3+}/\text{Fe}^{4+}$  during  $0.25 \leq x < 0.5$  in  $\text{Na}_{1-x}\text{FeO}_2$



**Figure S5.**  $\Delta G$  values for O@Fe-O-2Mn (blue) and O@2Fe-O-Mn (orange). Orange and blue shaded regions represent confidence interval 75% for values of O@Fe-O-2Mn and O@2Fe-O-Mn, respectively, indicating that the majority of  $\Delta G$  values for each oxygen site are highly localized within the confidence interval.



**Figure S6.** Averaged  $\Delta G$  of oxygen surrounded by various Fe oxidation numbers in the ground states of  $\text{Na}_{1-x}[\text{Mn}_{1/2}\text{Fe}_{1/2}]\text{O}_2$  at  $x = 0.75$  and  $0.875$ . To clearly compare the energy value with respect to the valence of surrounding Fe ions, the error bar is not included. Blue circles and orange circles present energy values for 2Fe–O–Mn and Fe–O–2Mn oxygen site. The blue and orange dashed boxes highlight that oxygen site classified by Fe coordination numbers can be further divided according to the valence states of surrounding Fe ions.

 $\text{O@2Fe-O-Mn}$  $\text{O@Fe-O-2Mn}$ 

**Figure S7.** The surrounding Na environment around oxygen having the  $\Delta G$  values used to calculate averaged  $\Delta G$  of  $\text{O@2Fe-O-Mn}$  and  $\text{O@Fe-O-2Mn}$  at  $x = 0.625$ . As shown in figure, all  $\text{O@2Fe-O-Mn}$  atoms are coordinated with adjacent Na atom, whereas, Na atoms are not presented around the majority of  $\text{O@Fe-O-2Mn}$  atoms (~67%).



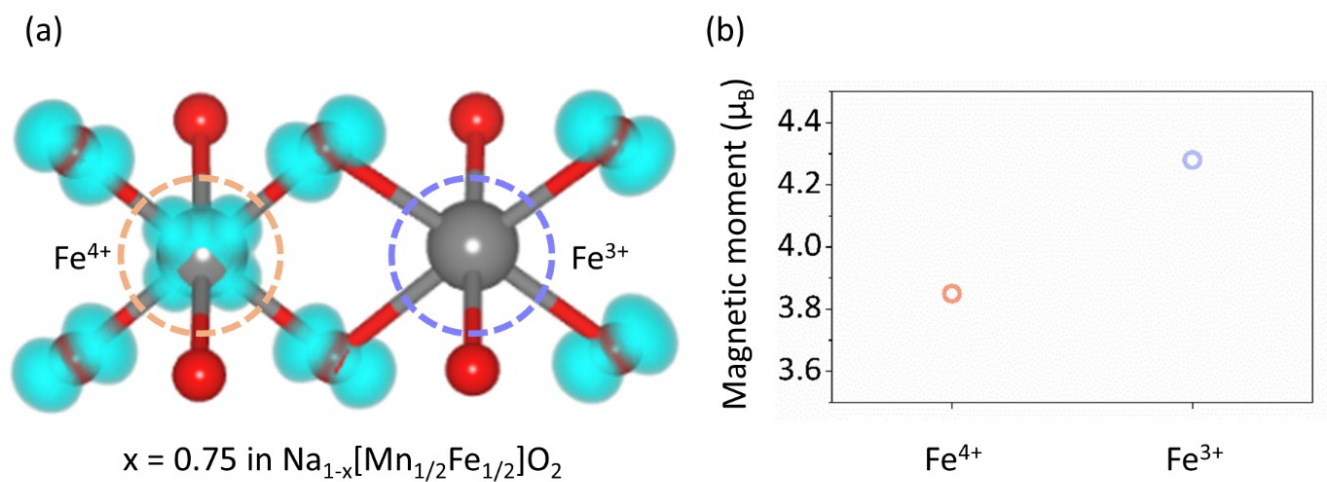


**Figure S8.** (a) Calculated spatial hole densities for Fe atoms at  $x = 0.75$  in  $\text{Na}_{1-x}[\text{Mn}_{1/2}\text{Fe}_{1/2}]\text{O}_2$ . Light orange and blue dashed circle represents  $\text{Fe}^{4+}$  and  $\text{Fe}^{3+}$  atoms, respectively. (b) Calculated magnetic moment of  $\text{Fe}^{4+}$  and  $\text{Fe}^{3+}$  ions. The calculated magnetic moment value of  $\text{Fe}^{3+}$  ( $\sim 4.3 \mu_B$ ) is well agreed to that of high-spin state of the  $\text{Fe}^{3+}$  ( $4.4 \mu_B$ ) ions, which was measured from neutron diffraction analysis.<sup>3</sup>

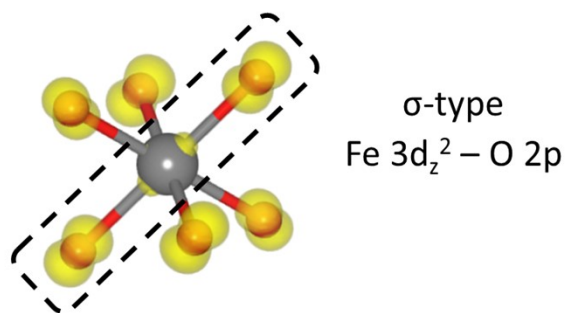


**Figure S9.** The spatial electron densities of  $\text{Fe}^{4+}\text{O}_6$  at  $x = 1.0$  in  $\text{Na}_{1-x}[\text{Mn}_{1/2}\text{Fe}_{1/2}]\text{O}_2$ , which was calculated in the energy range of  $-1.0 \leq E - E_f \leq 0.0$ . Yellow iso-surface represents electron densities. As shown in Figure S5,  $d_z^2$  orbital surrounds  $\text{Fe}^{4+}$  atom and is arranged toward O 2p orbital, which indicates  $\sigma$ -type Fe  $3d_z^2$ -O 2p molecular orbital.

## References

- 1 N. Yabuuchi, M. Kajiyama, J. Iwatate, H. Nishikawa, S. Hitomi, R. Okuyama, R. Usui, Y. Yamada and S. Komaba, *Nat. Mater.*, 2012, **11**, 512–517.
- 2 F. Tournadre, L. Croguennec, I. Saadoune, D. Carlier, Y. Shao-Horn, P. Willmann and C. Delmas, *J. Solid State Chem.*, 2004, **177**, 2790–2802.
- 3 M. Mekata, N. Yaguchi, T. Takagi, T. Sugino, S. Mitsuda, H. Yoshizawa, N. Hosoi and T. Shinjo, *J. Phys. Soc. Jpn.* 1993, **62**, 4474.